Methodology for Diagnostic Load Testing

Lantsoght, Eva; Bonifaz, J.; Sanchez, T.A.; Harris, D.K.

Publication date
2019

Document Version
Accepted author manuscript

Published in
Load Testing of Bridges

Citation (APA)
Lantsoght, E., Bonifaz, J., Sanchez, T. A., & Harris, D. K. (2019). Methodology for Diagnostic Load Testing. In E. Lantsoght (Ed.), *Load Testing of Bridges: Current Practice and Diagnostic Load Testing* (Vol. 12). CRC Press / Balkema - Taylor & Francis Group.

Chapter 8. Methodology for diagnostic load testing

E.O.L. Lantsoght

Politécnico, Universidad San Francisco de Quito, Quito, Ecuador & Concrete Structures, Delft University of Technology, Delft, the Netherlands

J. Bonifaz, T.A. Sanchez

ADSTREN Cía Ltda, Quito, Ecuador

D. K. Harris

Civil and Environmental Engineering, University of Virginia, Charlottesville, VA, USA

ABSTRACT: This chapter deals with the methodology for diagnostic load testing. All aspects of diagnostic load testing that are shared with other load testing methods have been discussed in Part II. In this chapter, the particularities of diagnostic load testing of new and existing bridges are discussed. These elements include loading procedures, monitoring behavior during the test, reviewing test data, calibrating analytical models, and evaluation of the test results.

1 INTRODUCTION

Load testing can be used to serve a number of purposes in bridge evaluation and is often referred to as either diagnostic or proof load testing (Lantsoght et al. 2017b). For new bridges, diagnostic load tests can demonstrate that the bridge behaves in the same way as it was designed (Kirkpatrick et al. 1984a, Kirkpatrick et al. 1984b, McGrath et al. 1995, Lawver et al. 2000, Barnes et al. 2003, Yang and Myers 2003, Ferrand et al. 2005, Konda et al. 2007, Harris et al. 2008, Au et al. 2013, Hernandez and Myers 2015, Harris et al. 2016, Taylor et al. 2016, Bonifaz et al. 2018, Hernandez and Myers 2018a). For this purpose, the measured responses during a field test are compared to the predicted responses obtained from the analytical model that was used for the design.

For existing bridges, diagnostic load tests can be used to evaluate certain aspects of the structural behavior and/or to calibrate the analytical model used for the assessment with field data in order to get an improved rating of the structure (Aktan et al. 1992, Saraf 1998, Al-Mahaidi et al. 2000, Velázquez et al. 2000, Jáuregui and Barr 2004, Hag-Elsafi and Kunin 2006, Mordak and

Manko 2008, Jeffrey et al. 2009, Hernandez and Myers 2016, Sanayei et al. 2016, Hernandez and Myers 2018b).

For both new and existing bridges, the aspects of structural behavior that can be determined in a diagnostic load testing include (Barker 2001):

- the actual impact factor or dynamic amplification factor (Hernandez and Myers 2018b) ,
- the stiffness of the total system including nonstructural elements that provide stiffness such as curbs and railings (Nilimaa et al. 2015),
- the internal system behavior of complex structural components (Harris et al. 2016),
- the actual stiffness after material deterioration,
- the transverse live load distribution (Arockiasamy and Amer 1997b, 1997a, 1998, Amer et al. 1999, Jones 2011, ACI Committee 342 2016, Ohanian et al. 2017),
- bearing restraint effects,
- the actual longitudinal live load distribution,
- load-bearing mechanisms that typically are not taken into account, such as arching action (Taylor et al. 2007),
- unintended or additional composite action, and
- effects of skew.

When these quantities are measured in the field and used for an improved assessment of an existing bridge, it is important to evaluate if it is conservative to assume that the quantity under consideration also acts at the load levels for which the bridge is assessed. For example, during a diagnostic load test, unintended composite action between steel girders and the concrete deck may be observed. However, at larger load levels, this composite action may be lost. Therefore, it is generally not rational to include effects such as unintended composite action or the restraint effects of frozen bearings that may be overcome at larger load levels in an assessment.

Diagnostic load tests can also be carried out on bridges after strengthening (Alkhrdaji et al. 2000, Russo et al. 2000, Bell and Sipple 2009, Myers et al. 2012, Au et al. 2013). To evaluate directly the effectiveness of strengthening measures, a diagnostic load test before and after applying strengthening can be performed and the relevant structural responses can be compared.

Since the goal of a diagnostic load test is to have a more realistic estimate of the actual properties of the bridge, diagnostic load testing can be carried out at lower load levels than the capacity of the bridge system. The applied load during the test should result in measurable responses that are appropriate to describe the operational state, i.e. the expected service response, but lower than that which would cause any permanent damage. As such, the required load during the test depends on the structural response under consideration, the intended behavior under evaluation, and may also depend on the accuracy of the available sensors. The requirements for implementation of diagnostic testing varies across the globe, with some government agencies requiring testing for initial acceptance of a new bridge, while others utilize testing primarily for evaluating structures after years of service. For example, Spanish guidelines (Ministerio de Fomento - Direccion General de Carreteras 1999) (see Part I) stipulate that for diagnostic load tests prior to opening of new bridges, the required loads must be representative of the design service load levels with a return period of 5 years. This load should cause around 60% of the ultimate limit state load effect and should never exceed 70% of the load effect at the ultimate limit state. These values can be taken as a reference during the preparation of a diagnostic load test. When service load levels are used for diagnostic load tests, and no nonlinear behavior is observed at these load levels, the same linear behavior is assumed for the loads the bridge needs to be designed or assessed for. On the contrary to this type of prescribed diagnostic testing, testing in the United States is often conducted on an ad-hoc basis to understand operational performance of existing bridges.

2 PREPARATION OF DIAGNOSTIC LOAD TESTS

2.1 New Bridge Diagnostic Testing

In general terms, the preparation of a diagnostic load test follows the steps described in Part II, Chapters 4 and 5. For a new bridge, an inspection is often recommended to identify differences between the design and as-built conditions. When relevant, the analytical model used for the design can be altered to reflect the as-built conditions. Then, the load paths and load levels for the diagnostic load test allow for exploration with the analytical model using load paths or load positions that result in the largest structural responses in the relevant structural members, or load paths that can be applied to have a range of responses required to meet the test objectives. As an example, the Los Pajaros Bridge (Ponton et al. 2016, LaViolette et al. 2017, Robalino and

Sanchez 2017, Sanchez et al. 2017, Bonifaz et al. 2018, Sanchez et al. 2018), a three-span steel bridge with cross-section shown in Figure 1, was diagnostically load tested following construction using the seven load cases shown in Figures 2-8. The material from the diagnostic load tests prior to opening of the Los Pajaros Bridge and the Villorita Bridge are used in this chapter to illustrate the general concepts explained here. Full examples of diagnostic load tests, detailing the preparation, execution, and post-processing of a load testing project, can be found in the next chapters. After determining the load paths, the target load level should be decided upon by verifying which number of loading vehicles results in measureable responses for the structural response under study and the available sensors.

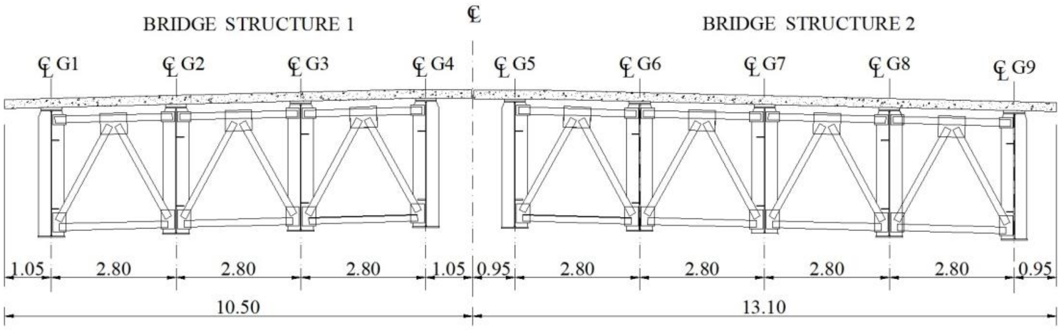

Figure 1. Cross-section of Los Pajaros Bridge, showing the two separate structures. Units: m. Conversion: 1 m = 3.3 ft.

For example, the Los Pajaros bridge was designed using the AASHTO LRFD code (AASHTO 2015); however, the bridge was part of the bridge network in Ecuador, which utilized the Spanish loading recommendation (Ministerio de Fomento - Direccion General de Carreteras 1999) of 60% of the design load. For this test, the target load for the diagnostic load test was estimated as follows. The bridge is design for the combination of the distributed lane load and one HL-93 truck, so the total design load can be calculated as follows: P_{1lane} = 9.36 kN/m × 195 m + 320 kN = 2145 kN (482 kip). For two lanes, P_{ULS} = 4290 kN (964 kip). Using 60% of the design load is then P_{target} = 2574 kN (579 kip). Each load case (see Figure 2 through Figure 8) consists of eight trucks of 294 kN (66 kip), resulting in a total load of 2352 kN (529 kip), which is close to the first estimate based on 60% of the design load. The trucks have axles distances of 1.6 m (5.2 ft) and 6 m (19.7 ft) and a distance between wheels in the transverse direction of 1.8 m (5.9 ft), see Figure 9. With the critical loading positions determined as discussed previously, and the total load and load per truck determined, the load cases (Figures 2-8) are fully defined:

- Load Case 1: Convoy of eight trucks in lanes 1 and 2 in span 1, center of convoy of trucks at midspan (0.54 L) for bridge structure 2.
- Load Case 2: Four trucks in lane 1 of span 1 and four trucks in lane 2 of span 2, center of trucks at midspan (0.54 L) of the respective spans.
- Load Case 3: Convoy of eight trucks in lanes 1 and 2 in span 2, center of convoy of trucks at midspan (0.54 L) for bridge structure 2.
- Load Case 4: Convoy of eight trucks in lanes 1 and 2 in span 3, center of convoy of trucks at midspan (0.46 L) for bridge structure 2.
- Load Case 5: Convoy of eight trucks in lanes 1 and 2 in span 3, center of convoy of trucks at midspan (0.46 L) for bridge structure 1.
- Load Case 6: Convoy of eight trucks in lanes 1 and 2 in span 2, center of convoy of trucks at midspan (0.54 L) for bridge structure 1.
- Load Case 7: Convoy of eight trucks in lanes 1 and 2 of span 1, center of convoy of trucks at midspan (0.54 L) for bridge structure 1.

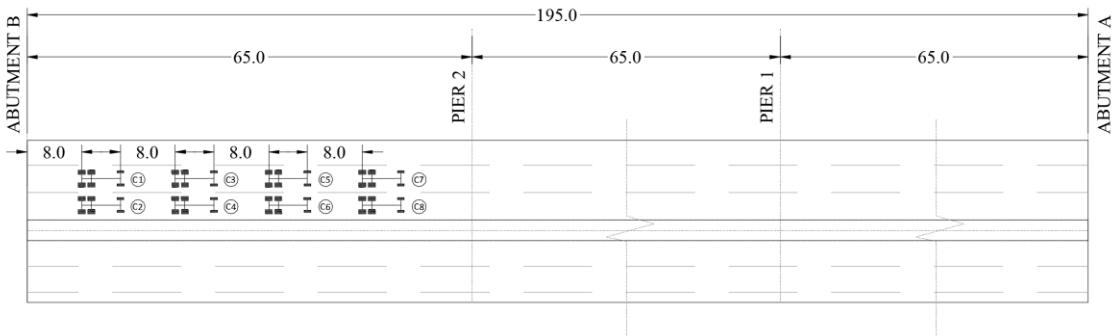

Figure 2. Load case 1 for Los Pajaros Bridge, Quito, Ecuador. Units: m. Conversion: 1 m = 3.3 ft.

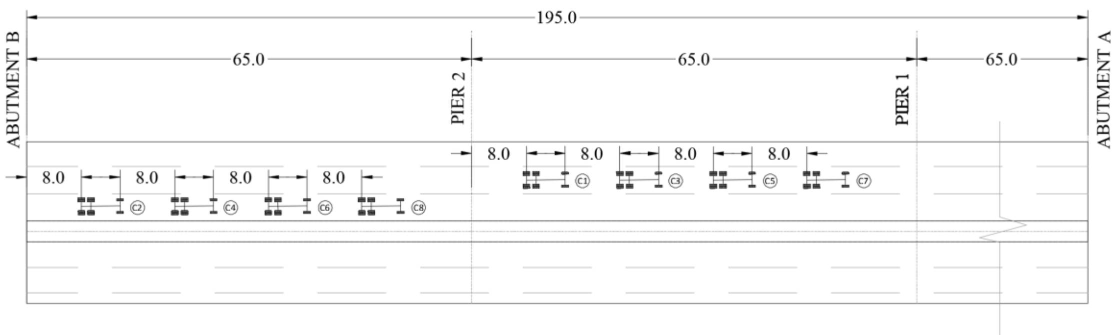

Figure 3. Load case 2 for Los Pajaros Bridge, Quito, Ecuador. Units: m. Conversion: 1 m = 3.3 ft.

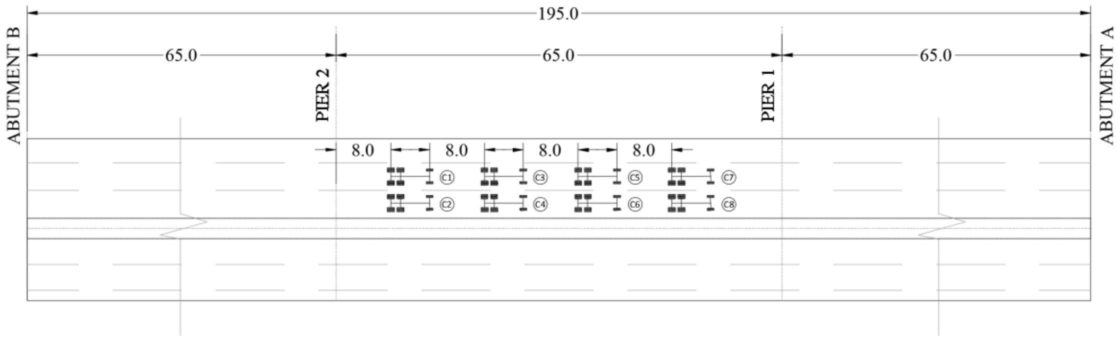

Figure 4. Load case 3 for Los Pajaros Bridge, Quito, Ecuador. Units: m. Conversion: 1 m = 3.3 ft.

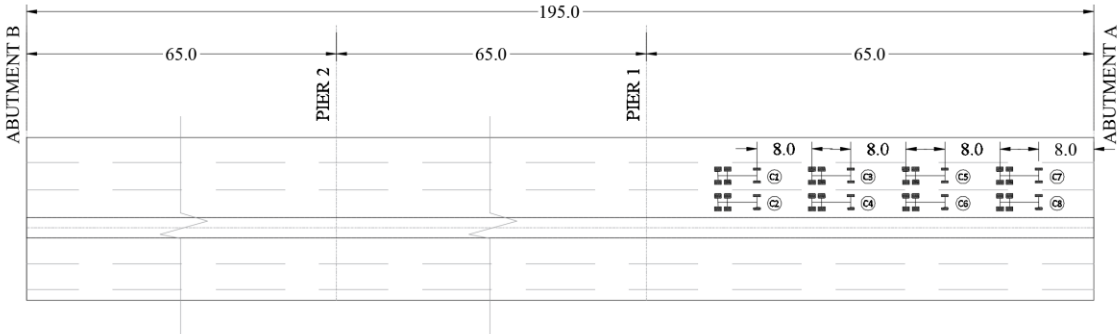

Figure 5. Load case 4 for Los Pajaros Bridge, Quito, Ecuador. Units: m. Conversion: 1 m = 3.3 ft.

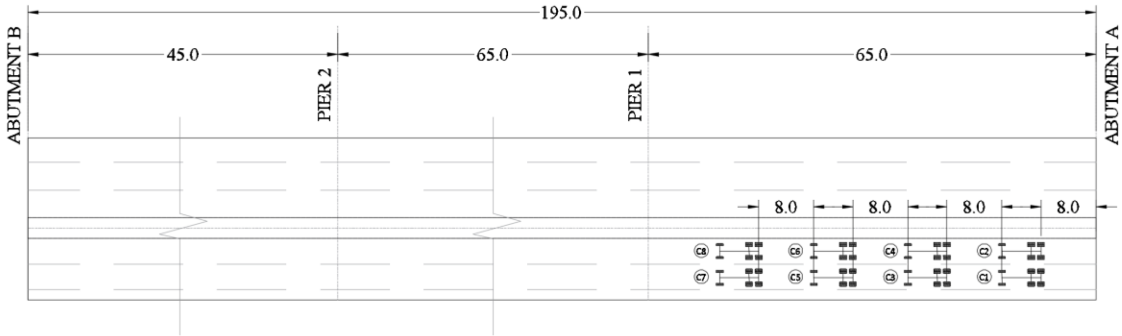

Figure 6. Load case 5 for Los Pajaros Bridge, Quito, Ecuador. Units: m. Conversion: 1 m = 3.3 ft.

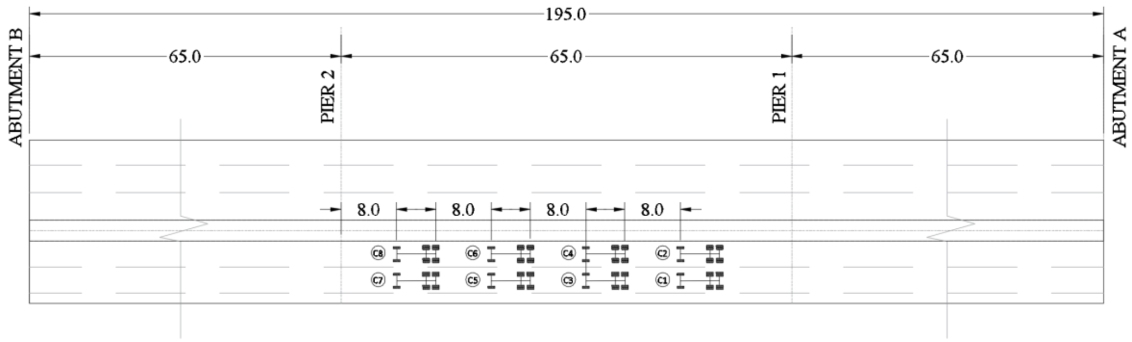

Figure 7. Load case 6 for Los Pajaros Bridge, Quito, Ecuador. Units: m. Conversion: 1 m = 3.3 ft.

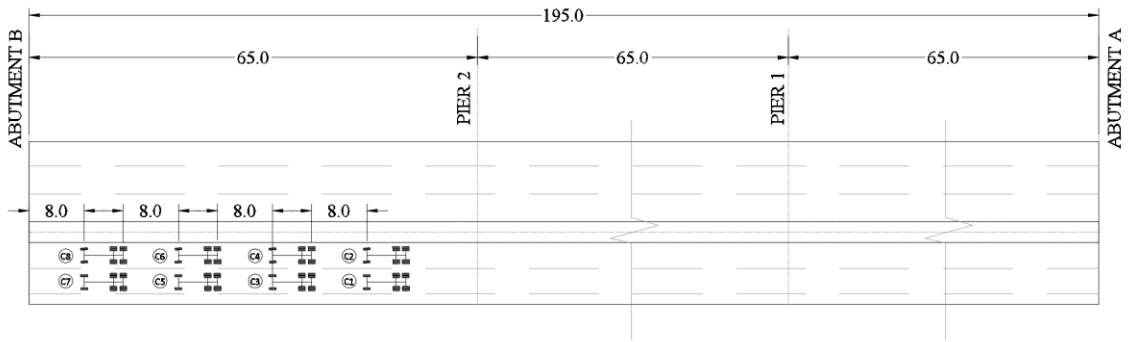

Figure 8. Load case 7 for Los Pajaros Bridge, Quito, Ecuador. Units: m. Conversion: 1 m = 3.3 ft.

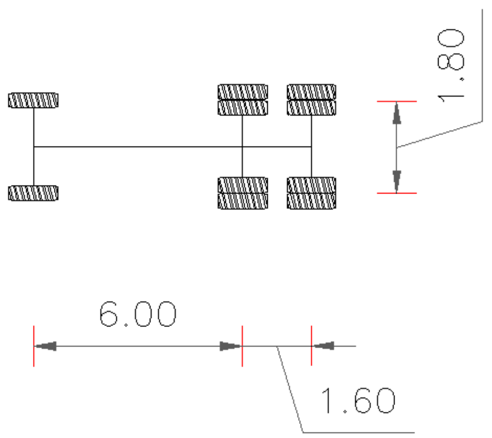

Figure 9. Configuration of trucks used for load test on Los Pajaros Bridge, Quito, Ecuador. Units: m. Conversion: 1 m = 3.3 ft.

The deflections for each load case were predicted using the linear finite element model that was used for the design. Figure 10 shows the graph of the predicted deflections of girder 6 for load case 4 on the Los Pajaros bridge.

After determining the load conditions for the test, the sensor plan can be developed. The most basic measurement consists of measuring deflections with a total station. This measurement is often sufficient for diagnostic load tests prior to opening new bridges; however other continuous sensor measurements (i.e. strain, displacement, rotation, and acceleration sensors) can be deployed depending on the intended measurement detail and resolution required. In addition, a planning for the on-site activities should be developed as well as a safety plan.

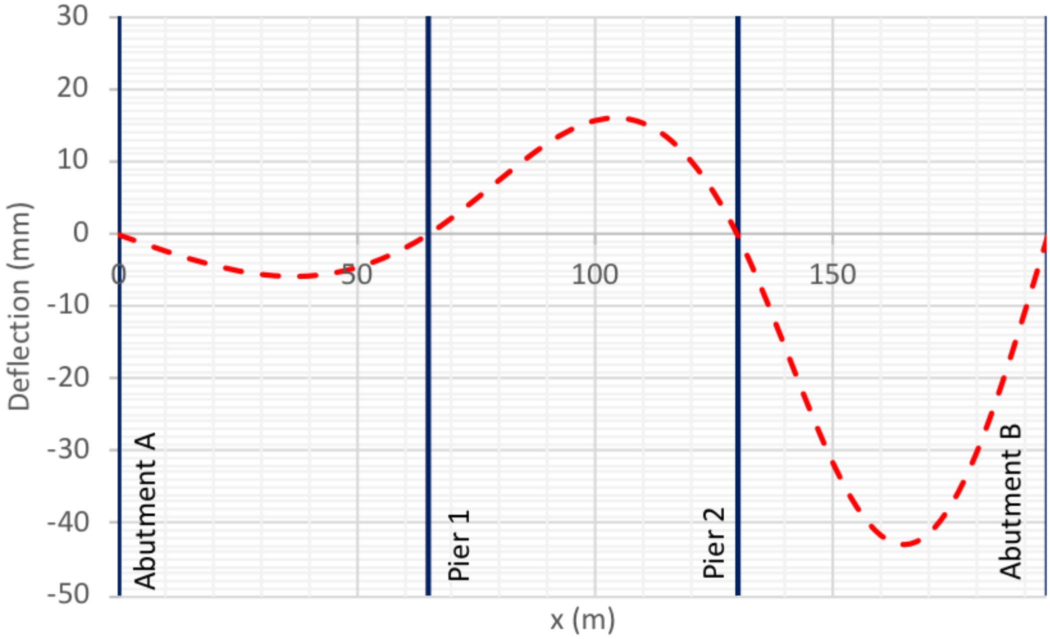

Figure 10. Predicted deflections for load case 4 on girder 6 of Los Pajaros Bridge. Conversion: 1 mm = 0.04 in, 1 m = 3.3 ft.

2.2 **Existing Bridge Diagnostic Testing**

For an existing bridge, the first step in a diagnostic test also typically includes a technical inspection. These inspections typically serve the purpose of identifying differences between the available plans (if any) and the actual conditions, identifying site limitations, and assessing the feasibility of the instrumentation plan. Changes to the (lane) layout, damage, deterioration, and material degradation should be reported and shown on updated drawings and damage maps. If an analytical rating prior to the test is not available, the necessary calculations should be done prior to the test. If the required input parameters regarding material properties and geometry are not known, they can be measured in the field as appropriate for the bridge type and material characteristics. For example:

- The geometry of the structure or even local features can be measured using basic surveying tools such as tape measure or total station (Hernandez and Myers 2018b), but can also be estimated using emerging technologies such as a laser scanner or Lidar unit.

- Material properties can often be determined through material sampling and/or non-destructive testing (Orban and Gutermann 2009), when appropriate.

- For concrete bridges, the positon and amount of reinforcement can be estimated with a rebar scanner or ground penetrating radar.

When the diagnostic test will be used to update the analytical model after the test to improve the rating of the bridge, the analytical model should be available prior to the test – either from previous rating calculations or as part of the preparation stage (Catbas et al. 2004, Jauregui et al. 2010, Hodson et al. 2013). If material deterioration or damage is observed during the inspection stage, these conditions need to be taken into account in the analytical model. To calculate the capacity for determining the Rating Factor (ratio of factored resistance for live load to factored live load demand) or Unity Check (ratio of factored load effect to design capacity as used in Europe), the effect of material deterioration and degradation also needs to be considered. For example, the effect of section loss in corroded steel members (Lim et al. 2016) or the reduction in shear capacity for concrete members suffering from alkali-silica reaction (den Uijl and Kaptijn 2004) should be taken into account in both the analytical model and diagnostic test results. Finally, the load path and target load are determined as described previously for new bridges. The remaining preparation steps include the development of the sensor plan, planning of the on-site activities, and safety plan.

3 PROCEDURES FOR THE EXECUTION OF DIAGNOSTIC LOAD TESTING

3.1 **Loading methods**

The loading methods available for load testing are described in Part II of this book as dead loads, loading vehicles, and systems with hydraulic jacks. In some cases, impact hammers/weights or electromagnetic shakers are often used for vibration testing, but this type of testing is beyond the scope of this chapter. For diagnostic load testing, the most common loading method is the use of loading vehicles, since the required loads are often representative of the typical service loads experienced by bridges. Additionally, these vehicular live loads are often more efficient with respect to deployment than static dead loads or loads applied via hydraulic jacks. Examples of using loading vehicles are given in Figure 11 for a steel girder bridge. Often in practice, various combinations of vehicle loading configurations are used depending on the intended loading magnitude required and design response observation. Another key advantage of using vehicular loading is that they can serve for both static and dynamic testing. Trucks can move at crawl speed or be placed at critical positions for a certain amount of time for static testing. Additionally for dynamic testing, trucks traveling at different speeds can be used to determine the dynamic amplification factor.

Figure 11. Diagnostic load test with loading vehicles on the Los Pajaros Bridge, Quito, Ecuador.

For static load tests, load cases are determined (see Figure 2 through 8). For diagnostic load testing at crawl speed or for moving trucks at a predetermined speed, load paths are determined. To couple the position of the loading vehicles to the measured structural responses, the position of the load should be known at all times. For this purposes, automated vehicle position trackers can be attached to a truck tire, or photogrammetry methods can be used. When photogrammetry methods are used and the vehicles are moving, the number of photographs that are taken per minute should be sufficiently large for the speed at which the vehicles are moving to capture the relevant information.

The advantage of the low load levels that are used in diagnostic load tests is that these tests can be carried out in a short amount of time (maximum one day). Diagnostic load tests can be carried out on one or more lanes of a bridge while other lanes remain in service, since typically there is no danger for the traveling public because of the low loads involved. To speed up the execution of a diagnostic load test, a standardized user interface that does not require programming (or only limited programming) can be combined with self-identifying sensors and a wireless sensor plan. Commercial solutions are available for standard diagnostic load testing procedures.

3.2 Monitoring bridge behavior during test

When a system with hydraulic jacks is used for loading the bridge, the output of the devices that measure the applied force (typically load cells) can be combined with the output of the applied sensors and processed in software to monitor the structural responses in real-time. When loading vehicles are used, the output of the vehicle trackers can be processed together with the measured structural responses for real-time evaluation. When photogrammetry methods are used to identify the truck positions, the data can be processed and visualized after each loading case. When there are concerns about the linearity of the bridge's behavior at the load levels used during the diagnostic load test, real-time data visualization and interpretation should be possible for safety reasons. For other cases, real-time data visualization is not required and an on-site check if the measured responses after the load test is sufficient.

It is common practice to compare the maximum deflection measured during a loading scenario to the analytically determined maximum deflection. Additionally, the residual deflection after the test is measured to see if the deflection returned to zero, see Figure 12. The measured residual deflection should be corrected for the effects of temperature and humidity to find the structural response due to the applied loading only. The influence of temperature and humidity on sensors and the measured structural responses is discussed in Part II.

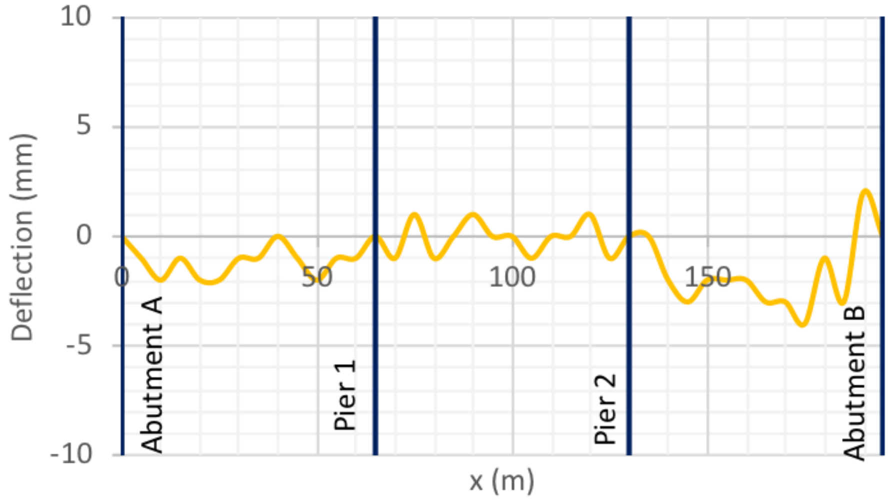

Figure 12. Results of measured deflections after unloading of Los Pajaros bridge, girder 6. Conversion: 1 mm = 0.04 in, 1 m = 3.3 ft.

Communication during the test between the test engineer and the operator of the load (when using hydraulic jacks) or the truck drivers (when using loading vehicles) is important and should be constant during the test. Cell phones or walkie-talkies can be used for this communication. The test engineer should be able to immediately communicate with the operator of the load or truck drivers when the measured structural responses show unexpected structural behavior and possible dangerous situations.

4 PROCESSING DIAGNOSTIC LOAD TESTING RESULTS

4.1 **On-site validation and review of test data**

After each load case, the measured data should be reviewed, see Figure 13. For static tests, longitudinal and transverse deflection plots can be generated. For dynamic tests, the data can be reviewed by plotting the time and load histories of the sensors. This review serves the purpose of detecting sensor malfunctioning and detecting possible dangerous behavior of the structure during the test. If the review shows sensor malfunctioning, the sensor can be replaced and the load case can be repeated. If the review shows indications of possible dangerous behavior, the testing should be interrupted and the structural behavior should be further investigated. In these cases, the critical elements should be inspected if possible and if it can be done in a safe way.

The data need to be reviewed for symmetry, repeatability, and linearity. For symmetric load configurations, the resulting structural responses should be symmetric. Figure 14 shows an example of a load test where this requirement is fulfilled. For repeated load cases and load levels, the measured structural responses should be the same. Finally, when increasing load levels are used, the measured structural responses should increase linearly with the increase in load.

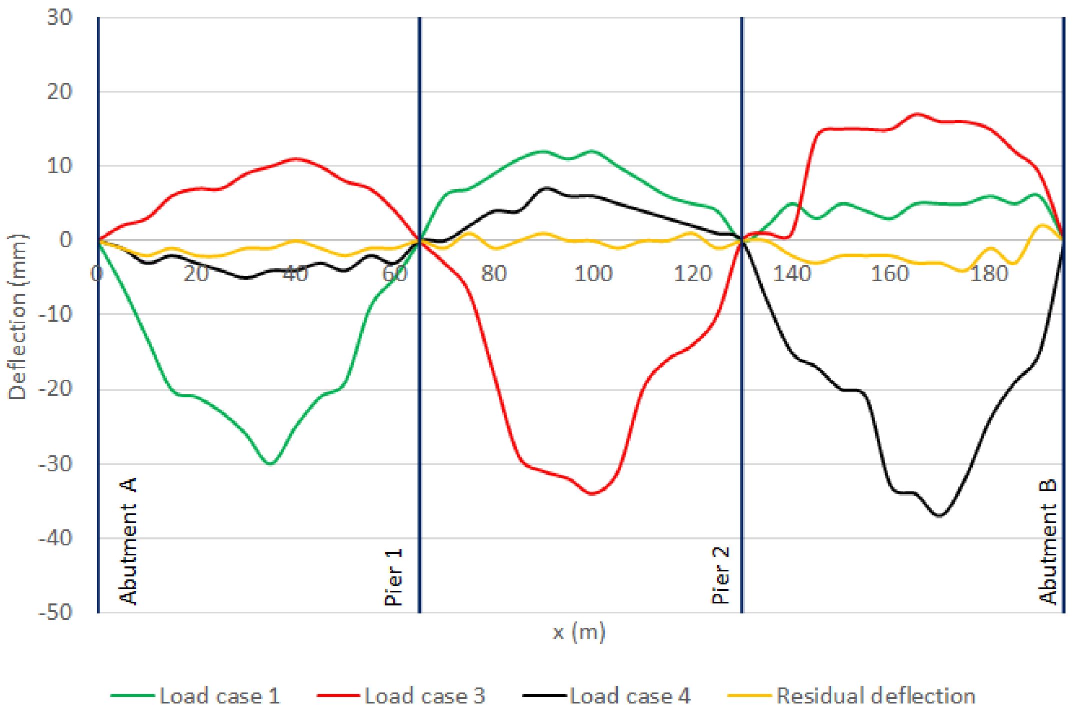

Figure 13. Review of different load cases for girder 6 of Los Pajaros Bridge. Conversion: 1 mm = 0.04 in, 1 m = 3.3 ft.

When all load is removed, the residual deformations should be small, see for example Figure 12. When reviewing the data for symmetry, repeatability, and linearity, the environmental effects on the measured structural responses should be filtered out. Additionally, depending on the construction material, there may be time-dependent effects in the material that influence the measured structural responses. The time-dependent effects can be assessed by reporting the residual deformations after unloading. Where necessary and interesting, the measurements can remain activated for up to 24 hours to measure the reduction of the residual deformations as a function of the time. Time-dependent effects may need to be considered in concrete, timber, masonry, and plastic composite bridges.

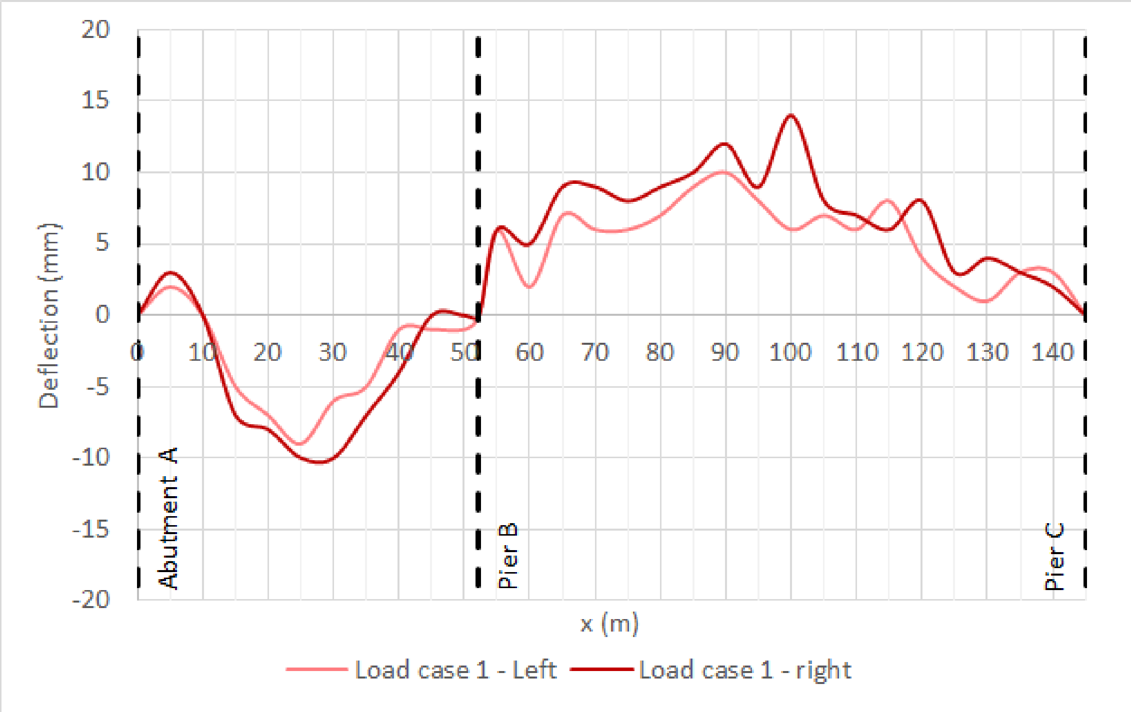

Figure 14. Symmetry of load cases left and right for Villorita Bridge in Quito, Ecuador. Conversion: 1 mm = 0.04 in, 1 m = 3.3 ft.

Possible problems with the sensor output are: large amounts of noise when the structural responses are small relative to the measurement range of the sensor, a shift in the measurements caused by hitting of the sensor or wires, constant output when a sensor is outside of its range, and noise effects when the transducer attachment is not functioning properly, or when electromagnetic radiation interferes with the measurements.

4.2 **Processing and reporting test data**

After the diagnostic load test, the measured responses should be corrected for additional influences. For example, strain measurements may need to be compensated for the effects of temperature and humidity, and deflection measurements may need to be corrected with support deflections to find the net deflection of the structure for comparison to the analytical models. The effect of temperature and humidity on sensors and structural responses is discussed in Part II. However, since diagnostic load tests typically are carried out during a short amount of time and either using moving vehicles or keeping vehicles for a short amount of time on one position, the time of a load cycle is typically short and these environmental factors are expected have minimal impact on the results of any given loading repetition, but could impact responses across loading repetitions.

The raw data should be evaluated for issues such as a sensor running out of its measurement range, and spikes in the measurements that have no structural explanation and are erroneous. Where necessary, the data should be processed by applying a noise filter (Lin et al. 2018).

Then, the processed time histories should be compared to the values obtained from the analytical model (Harris et al. 2015). This initial comparison of the field output and the analytical model can be used to identify major differences between the assumptions in the analytical model and the actual bridge behavior. Based on this comparison, the test engineer may be able to identify which parameters need to be adjusted in the analytical model.

After processing of the data, the following plots –depending on the structural responses that were measured during the test and that are necessary to meet the goals of the test- can be generated for inclusion in the test report:

- the sensor output as a function of the time for each sensor (similar responses can be combined in one figure),
- the sensor output as a function of the applied load for each sensor (similar responses can be combined in one figure),
- the applied loading schemes (plot of time versus load) when hydraulic jacks are used, or the load levels and load configurations when loading vehicles are used (drawings of positions and table of measured weights of the vehicles),
- longitudinal and transverse deflection profiles for the different load levels or load configurations that were applied,
- strain profiles measured over the height of girders or at critical locations.

4.3 **Verification of structural responses for new bridges**

For new bridges, the structural responses obtained during the test and reported as discussed in section 4.2 should be compared to the predicted structural responses from the analytical model. It is often common practice to illustrate the predicted relative to the tested structural responses; these comparisons serve as a mechanism to evaluate the validity of the analytical model used for the design of the bridge, and hence the overall performance of the bridge. Possible outcomes derived from this comparison are further discussed in §5.1. Based on this comparison and the evaluation of the tested and predicted responses, the test engineer will be able to give guidance to an owner on whether or not it is safe to open the new bridge to traffic.

4.4 **Calibration of analytical model for existing bridges**

For any bridge, the general assumption is that analytical model represents an approximation of the structural behavior and the experimental measurements serve as the ground truth. The convergence of these two mechanisms can be achieved through model calibration, which aims to improve a model's approximation by updating with better representations of in-situ conditions (e,g, constitutive properties, boundary condition, composite behavior, secondary member contribution, deterioration, etc.). In the literature, there are numerous studies that explore this calibration; however, a generalized and systematic approach presented by Barker (Barker 2001) is considered herein. This method was developed for bridge with steel-concrete composite sections, but can be easily adapted for other building material or sections. This method is summarized here, and follows a number of steps:

1. Inspection of the bridge to quantify the actual dimensions and dead loads, and resulting stresses due to dead load σ_D. This step is carried out during the preparation stage of the load test.
2. Calculate the experimental impact factor resulting from the diagnostic load test I_{mE}.
3. Calculate the experimental distribution factors DF_E.
4. Determine the bearing restraint moments M_{BR}.
5. Remove axial stresses from the stress profiles for steel members.
6. Calculate the total measured moment M_T.
7. Remove the bearing restraint moments M_{BR} from the total measured moment M_T to find the elastic moments M_E.
8. Calculate the experimental section moduli S_E.
9. Calculate the elastic longitudinal adjustment moments M_{LE}.
10. Determine the experimental rating factor.

Details on how to calculate the experimental rating factor according to Barker's method are given in Appendix A. Another, more general approach, is the method described in the AASHTO MBE (AASHTO 2016) and the Manual for Bridge Rating through Load Testing (NCHRP 1998), where the rating factor is updated based on the ratio of tested to predicted strain, and corrected for the frequency of inspection, the ability of the test team to identify difference between the tested and predicted responses, and the presence of fatigue- or fracture-critical features. The reader can find this approach presented and discussed in Chapter 3.

When a finite element model is used for the assessment of an existing bridge, it can be calibrated with the responses measured in the field (Bridge Diagnostics Inc. 2012). The methods presented in this section can be used together with ratings based on a finite element model. When the calibration is carried out with a finite element model, the different properties that are mentioned in the section can be varied until a combination of parameters is found that best represents the field results. This calibration is carried out by applying the trucks used in the field test on the finite element model and reading out the structural responses due to static live load effects only (Hernandez and Myers 2016, Hernandez 2018). For easy comparison between the model and the test results, the finite element model should have nodes at the positions of the measurements. Mathematically, the best representation can be expressed in terms of the smallest error (for example based on a least-squares approach (Bridge Diagnostics Inc. 2012)) between the finite element model and the field test results. In practice, however, the optimization of the finite element model is an iterative procedure, in which optimization methods are combined with engineering judgement. The test engineer here needs to identify which parameters should be optimized, and what are the reasonable limits for these values.

When nonlinear structural responses are observed during the diagnostic load test, linear finite element models are not recommended for the assessment, and the step to nonlinear modelling should be made or the loads on the bridge should be limited to the linear range.

5 EVALUATION OF DIAGNOSTIC LOAD TESTING RESULTS

5.1 Evaluation of results for new bridges

Depending on the governing code or guidelines, for new bridges it is sufficient to show with a diagnostic load test that the bridge behaves as designed. Often, the field measurements will show that the design assumptions are conservative. If the measured structural responses exceed the expected responses (by between 10% and 20%, depending on the governing code and the construction material, see Chapter 3), the cause for this difference needs to be identified. In that case, it may be necessary to update the analytical model and verify the design calculations. Re-testing may be necessary. In summary, for new bridges, three outcomes are possible after a diagnostic load test:

1. The predicted structural response is larger than the measured structural response. The analytical model used for the design is thus on the conservative side, and no further actions are necessary.

2. The predicted structural response is more or less equal to the measured structural response. The analytical model used for the design is a good representation of the structural behavior. No further actions are necessary.

3. The predicted structural response is smaller than the measured structural response. The analytical model is not conservative. The test engineer, owner, and designer should meet to decide on the further actions.

For the first case, when it is found that the analytical model is conservative, the owner may request the designer to update the analytical models used for the design to have a model that predicts the new bridge as closely as possible. This model can then be used in the future for assessments, and can be updated to take into account changes to the structure or material deterioration/degradation. These changes could be based on material sampling, non-destructive testing, and future diagnostic load tests. The methods for updating an analytical model after a diagnostic load test are discussed in §4.4 and how to use the updated model for an assessment is discussed in §5.2. Figure 15 shows an example of a case where the analytical model of a rather flexible bridge is on the conservative side.

The second case is the ideal case, in which the analytical model closely predicts the structural responses measured during the test. It is good practice to transfer this analytical model from the designer to the bridge owner or the responsible party for the operation, management, and maintenance of the bridge, so that the model can be used for future assessments and in combination with future load tests. Figure 16 and Figure 17 show the results for maximum sagging and maximum hogging deflection, respectively, for girder 6 of the Los Pajaros Bridge. For this case, the measured deflection of 37 mm (1.5 in) was 86% of the predicted deflection of 43 mm (1.7 in) for the maximum sagging deflection. For the maximum hogging deflection, the measured deflection of 17 mm (0.7 in) was 106% of the predicted deflection of 16 mm (0.6 in).

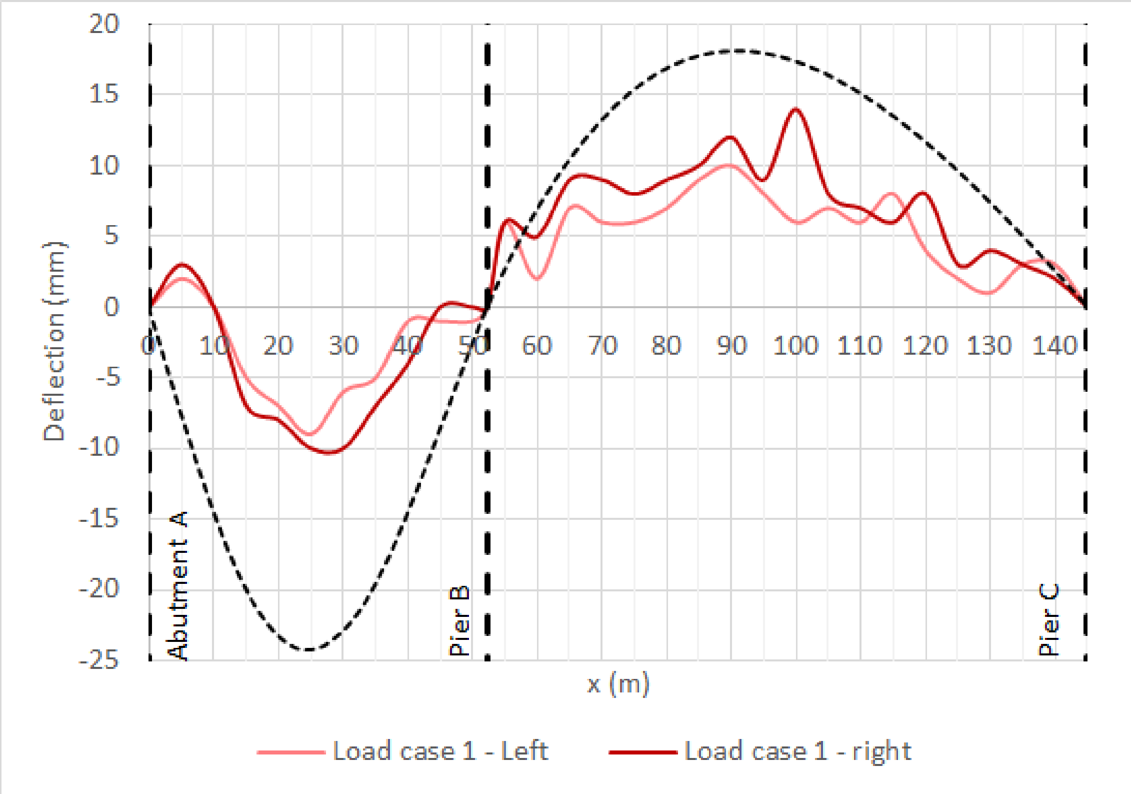

Figure 15. Example of difference between analytically determined maximum deflection and measured maximum deflection for flexible structure. Conversion: 1 mm = 0.04 in, 1 m = 3.3 ft.

The third case, in which the analytical model predicts smaller structural responses than the responses measured in the field, is typically addressed by limits to the ratio of tested to predicted response in the existing codes and guidelines (see Chapter 3). Where no such limits are available, they should be agreed upon prior to the diagnostic load test in accordance between the owner, test engineer, and designer. When these limits are exceeded, the following actions or a combination thereof can be proposed:

- visual inspection directly after the diagnostic load test, to identify possible signs of distress,
- on-site inspection of the bearings,
- material sampling or non-destructive testing of the bridge's materials,
- reevaluation of the analytical model by the designer or by a third party,
- repeat diagnostic load test.

The first step is often a visual inspection to identify possible signs of distress that may have resulted in the larger than expected structural responses. If no signs of distress are observed, the bearings and/or material properties can be checked. If the bridge is in an acceptable condition and the materials and bearings are as designed, then the analytical model should be reevaluated – either by the designer or by a third party. If errors in the analytical model are found, a full assessment of the safety of the bridge should be carried out before the bridge can be deemed safe to open to the traffic. A new analytical model may need to be developed, and a repeat diagnostic load test may be necessary.

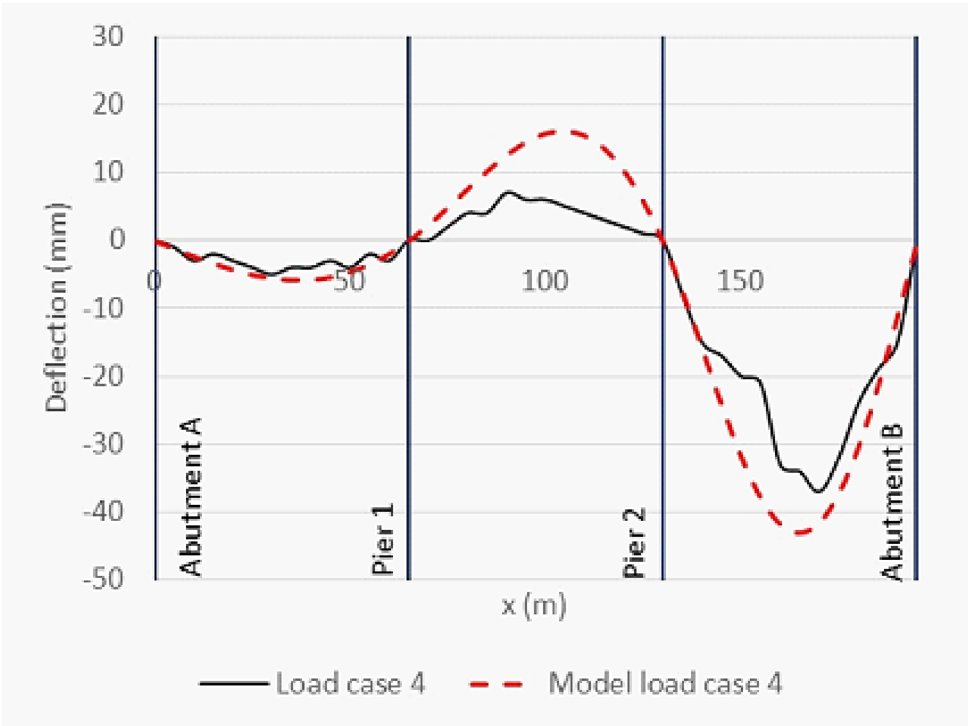

Figure 16. Comparison between analytically determined deflections and predicted deflections for girder 6 of Los Pajaros bridge for the case that causes maximum sagging deflection. Conversion: 1 mm = 0.04 in, 1 m = 3.3 ft.

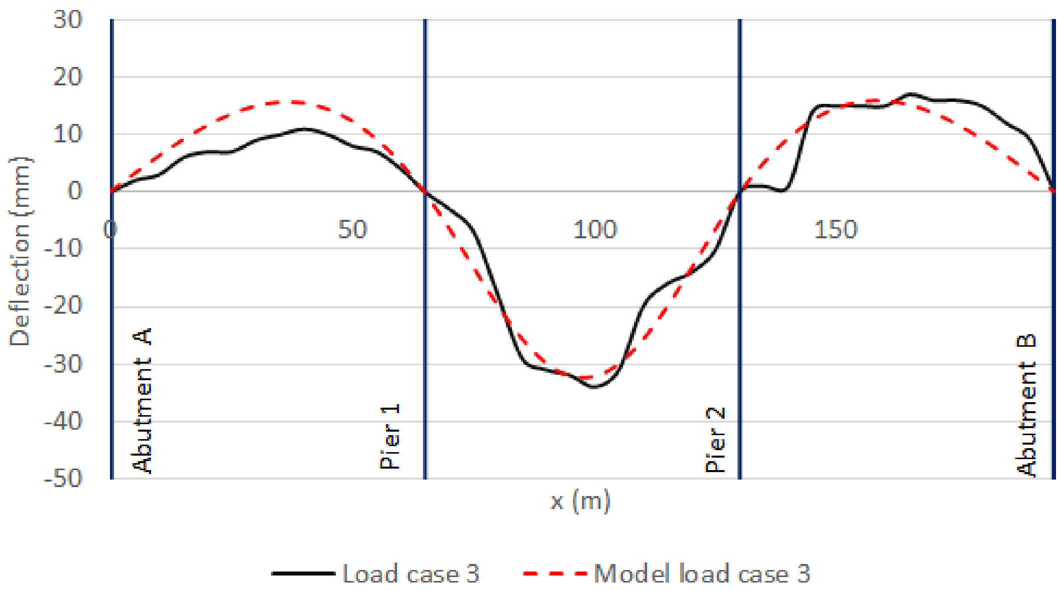

Figure 17. Comparison between analytically determined deflections and predicted deflections for girder 6 of Los Pajaros bridge for the case that causes maximum hogging deflection. Conversion: 1 mm = 0.04 in, 1 m = 3.3 ft.

5.2 **Improved assessment for existing bridges**

For existing bridges, the responses measured during the field test can be used (depending on the goals of the test) to calibrate the analytical models used for the original rating of the bridge, as discussed in §4.2. The updated model is then used to determine the corresponding rating, which reflects the actual performance of the bridge at a given moment during its service life (Wipf et al. 2000). Typically, the loads applied during a diagnostic load test are not the loads required for the assessment. Therefore, in the updated analytical model, the trucks applied during the diagnostic load test are removed, and the loads required for the assessment are applied. Different scenarios, such as inventory and operating rating levels according to the Manual for Bridge Evaluation (AASHTO 2016) in North America, superloads that may need to pass the bridge, or different load levels calibrated for different reliability indices as used in the Netherlands (Rijkswaterstaat 2013), can then be evaluated with the updated model. For these assessment calculations, the critical loading position in the longitudinal and transverse direction should be determined for each load model applied to the analytical model. Depending on the lane layout of the bridge, the assessment should include design trucks or tandems in all lanes and pattern loading across the spans.

As for all load tests, and as highlighted in Part II, the influence of the diagnostic load test on the assessment lies on the side of the live load effects. When a rating factor is calculated, the diagnostic load test serves to update the load effect due to the live loads. When a Unity Check is calculated, the diagnostic load test serves to update the load effect due to the considered load combination. The diagnostic load test gives no information about the capacity of the considered section for the failure mode of interest. For the assessment calculations, the capacity is determined based on the governing code equations, and the effect of material degradation and section losses should be taken into account. In special cases, more elaborate models for the capacity can be used, so that additional sources of capacity that are not included in the simplified code equations can be taken into account. An example is the use of the Extended Strip Model for the determination of the maximum load on reinforced concrete slab bridges (Lantsoght et al. 2017a).

When the different relevant scenarios are evaluated with the updated model and the resulting Rating Factors (in North America) or Unity Checks (in Europe) are obtained, recommendations can be given. If the Rating Factors for all relevant rating levels are larger than one or if the Unity Checks for the relevant load levels are smaller than one, no actions are necessary. If the Rating Factors are smaller than one or the Unity Checks are larger than one, the following recommendations can be given:

- carrying out a proof load test (if it is expected that such a test could demonstrate adequate performance at higher load levels),
- posting of the bridge (NCHRP 2014),
- strengthening the bridge, or
- demolishing and replacing the bridge.

For such bridges, permits for superloads should be carefully evaluated when requested. The engineer responsible for the diagnostic load test can only give a recommendation to the bridge owner; the final management decision lies with the bridge owner.

6 SUMMARY AND CONCLUSIONS

This chapter describes the general methodology that can be followed for diagnostic load tests on new and existing bridges. For new bridges, diagnostic load tests can be required prior to opening the bridge. For existing bridges, diagnostic load tests can be used to have a better understanding of the overall structural behavior, and/or to improve the analytically determined assessment of the bridge.

For diagnostic load tests, the preparation stage involves the determination of the required magnitude of the load during the test, the loading positions (for static load tests) and/or the load paths (for dynamic load tests). The applied load should be large enough to result in measurable structural responses. The preparation stage also involves the development of the sensor plan, planning of on-site activities, and safety plan.

During the load test, and depending on the type of load test, it may be necessary to follow the responses in real time, or after each load case or load path. Communication between the load operators or truck drivers and the testing engineers is important during the execution stage.

After the load test, a first on-site check of the measured structural responses is required. The quality of the data should be checked. The measured structural behavior should be checked in terms of repeatability, symmetry, and linearity of the measured responses. Then, a first comparison to the analytically determined responses should be done. If there are doubts regarding the structural behavior or if possible sensor malfunctioning is identified, a load case or load path can be repeated at that moment. The complete post-processing of the measurement data happens in the office after finishing all on-site activities. This post-processing includes correcting the data for environmental effects, finding net deflections where necessary, and filtering out erroneous measurement results. These processed data will then be shown in the measurement report, and can be used to calibrate the available analytical models. For new bridges, such calibration may not be required. For existing bridges, the calibrated analytical model can be used to obtain a more realistic assessment, taking into account the actual bridge behavior measured in the field.

REFERENCES

AASHTO 2015. *AASHTO LRFD bridge design specifications, 7th edition with 2015 interim specifications,* Washington, DC, American Association of State Highway and Transportation Officials.

AASHTO 2016. *The manual for bridge evaluation with 2016 interim revisions,* Washington, D.C., American Association of State Highway and Transportation Officials.

ACI COMMITTEE 342 2016. ACI 342R-16: Report on Flexural Live Load Distribution Methods for Evaluating Exisiting Bridges. Farmington Hills, Michigan: American Concrete Institute.

AKTAN, A. E., ZWICK, M., MILLER, R. & SHAHROOZ, B. 1992. Nondestructive and Destructive Testing of Decommissioned Reinforced Concrete Slab Highway Bridge and Associated Analytical Studies. *Transportation Research Record: Journal of the Transportation Research Board,* 1371**,** 142-153.

AL-MAHAIDI, R., TAPLIN, G. & GIUFRE, A. 2000. Load Distribution and Shear Strength Evaluation of an Old Concrete T-Beam Bridge. *Transportation Research Record,* 1696**,** 52-62.

ALKHRDAJI, T., NANNI, A. & MAYO, R. 2000. Upgrading Missouri Transportation Infrastructure - Solid Reinforced-Concrete Decks Strengthened with Fiber-Reinforced Polymer Systems. *Transportation Research Record,* 1740**,** 157-163.

AMER, A., AROCKIASAMY, M. & SHAHAWY, M. 1999. Load distribution of existing solid slab bridges based on field tests. *Journal of Bridge Engineering,* 4**,** 189-193.

AMERICAN ASSOCIATION OF STATE HIGHWAY AND TRANSPORTATION OFFICIALS 2011. *The manual for bridge evaluation,* Washington, D.C., American Association of State Highway and Transportation Officials.

AROCKIASAMY, M. & AMER, A. 1997a. Load Distribution on Highway Bridges Based On Field Test Data: Phase I.

AROCKIASAMY, M. & AMER, A. 1997b. Load Distribution on Highway Bridges Based On Field Test Data: Phase II.

AROCKIASAMY, M. & AMER, A. 1998. Load Distribution on Highway Bridges Based On Field Test Data: Phase III.

AU, A., LAM, C., AU, J. & THARMABALA, B. 2013. Eliminating Deck Joints Using Debonded Link Slabs: Research and Field Tests in Ontario *Journal of Bridge Engineering,* 18**,** 768-778.

BARKER, M. G. 2001. Quantifying Field-Test Behavior for Rating Steel Girder Bridges. *Journal of Bridge Engineering,* 6**,** 254-261.

BARNES, R. W., STALLINGS, J. M. & PORTER, P. W. 2003. Live-Load Response of Alabama's High-Performance Concrete Bridge. *Transportation Research Record,* 1845**,** 115-124.

BELL, E. S. & SIPPLE, J. D. 2009. Special topics studies for baseline structural modeling for condition assessment of in-service bridges. *Safety and Reliability of Bridge Structures.*

BONIFAZ, J., ZARUMA, S., ROBALINO, A. & SANCHEZ, T. A. 2018. Bridge Diagnostic Load Testing in Ecuador – Case Studies. *IALCCE 2018.* Ghent, Belgium.

BRIDGE DIAGNOSTICS INC. 2012. Integrated Approach to Load Testing.

CATBAS, F. N., CILOGLU, S. K. & AKTAN, A. E. 2004. Strategies for load rating of infrastructure populations: a case study on T-beam bridges. *Structure and Infrastructure Engineering,* 1**,** 221-238.

DEN UIJL, J. A. & KAPTIJN, N. 2004. Structural consequences of ASR: an example on shear capacity. *Heron,* 47**,** 1-13.

FERRAND, D., NOWAK, A. S. & SZERSZEN, M. M. 2005. Field Test and Finite Element Analysis of Isotropic Bridge Deck. *Transportation Research Record,* CD 11-S**,** 153-158.

HAG-ELSAFI, O. & KUNIN, J. 2006. Load Testing For Bridge Rating: Dean's Mill Road Over Hannacrois Creek. Albany, NY: Transportation Research and Development Bureau, New York State Department of Transportation.

HARRIS, D. K., CIVITILLO, J. M. & GHEITASI, A. 2016. Performance and Behavior of Hybrid Composite Beam Bridge in Virginia: Live Load Testing. *Journal of Bridge Engineering,* 21**,** 04016022.

HARRIS, D. K., COUSINS, T., MURRAY, T. M. & SOTELINO, E. D. 2008. Field Investigation of a Sandwich Plate System Bridge Deck. *Journal of Performance of Constructed Facilities,* 22**,** 305-315.

HARRIS, D. K., GHEITASI, A. & CIVITILLO, J. M. 2015. Field testing and numerical modeling of a hybrid composite beam bridge in Virginia. *European Bridge Conference.* Edinburgh, UK.

HERNANDEZ, E. S. 2018. *Service response and evaluation of prestressed concrete bridges through load testing.* Ph.D., Missouri University of Science and Technology.

HERNANDEZ, E. S. & MYERS, J. J. 2015. In-situ field test and service response of Missouri Bridge A7957. *European Bridge Conference.* Edinburgh, UK.

HERNANDEZ, E. S. & MYERS, J. J. 2016. Initial in-service response and lateral load distribution of a prestressed self-consolidating concrete bridge using field load tests. *In:* BAKKER, J., FRANGOPOL, D. M. & BREUGEL, K. V. (eds.) *The Fifth International Symposium on Life-Cycle Civil Engineering (IALCCE 2016).* Delft, The Netherlands: CRC Press.

HERNANDEZ, E. S. & MYERS, J. J. 2018a. Diagnostic Test for Load Rating of a Prestressed SCC Bridge. *ACI Special Publication,* 323.

HERNANDEZ, E. S. & MYERS, J. J. 2018b. Strength evaluation of prestressed concrete bridges by dynamic load testing. *Ninth International Conference on Bridge Maintenance, Safety and Management (IABMAS 2018).* Melbourne, Australia: CRC Press.

HODSON, D. J., BARR, P. J. & POCKELS, L. 2013. Live-Load Test Comparison and Load Ratings of a Posttensioned Box Girder Bridge. *Journal of Performance of Constructed Facilities,* 27**,** 585-593.

JÁUREGUI, D. V. & BARR, P. J. 2004. Nondestructive Evaluation of the I-40 Bridge over the Rio Grande River. *Journal of Performance of Constructed Facilities,* 18**,** 195-204.

JAUREGUI, D. V., LICON-LOZANO, A. & KULKARNI, K. 2010. Higher Level Evaluation of a Reinforced Concrete Slab Bridge. *Journal of Bridge Engineering,* 15**,** 172-182.

JEFFREY, A., BREÑA, S. F. & CIVJAN, S. A. 2009. Evaluation of Bridge Performance and Rating through Nondestructive Load Testing. University of Massachusetts Amherst.

JONES, B. P. 2011. *Reevaluation of the AASHTO effective width equation in concrete slab bridges in Delaware.* MSc. Thesis, University of Delaware.

KIRKPATRICK, J., LONG, A. E. & THOMPSON, A. 1984a. Load distribution characteristics of spaced M-beam bridge decks. *The structural engineer,* 62B**,** 86-88.

KIRKPATRICK, J., RANKIN, G. I. B. & LONG, A. E. 1984b. Strength evaluation of M-beam bridge deck slabs. *The structural engineer,* 62B**,** 60-68.

KONDA, T. F., KLAIBER, F. W., WIPF, T. J. & SCHOELLEN, T. P. 2007. Precast Modified Beam-in-Slab Bridge System - An Alternative Replacement for Low-Volume Roads. *Transportation Research Record,* 1989**,** 335-346.

LANTSOGHT, E. O. L., VAN DER VEEN, C., DE BOER, A. & ALEXANDER, S. D. B. 2017a. Extended Strip Model for Slabs under Concentrated Loads. *ACI Structural Journal,* 114**,** 565-574.

LANTSOGHT, E. O. L., VAN DER VEEN, C., HORDIJK, D. A. & DE BOER, A. 2017b. State-of-the-art on load testing of concrete bridges. *Engineering Structures,* 150**,** 231-241.

LAVIOLETTE, M., SANCHEZ, T. A. & FIALLO, M. 2017. Construction of Ecuador's First Launched Steel Girder Bridge. *Proceedings, National ABC Conference, Florida International University.* Miami, FL.

LAWVER, A., FRENCH, C. & SHIELD, C. K. 2000. Field Performance of Integral Abutment Bridge. *Transportation Research Record,* 1740**,** 108-117.

LIM, S., AKIYAMA, M. & FRANGOPOL, D. M. 2016. Assessment of the structural performance of corrosion-affected RC members based on experimental study and probabilistic modeling. *Engineering Structures,* 127**,** 189-205.

LIN, W., TANIGUCHI, N., YODA, T., HANSAKA, M., SATAKE, S. & SUGINO, Y. 2018. Renovation of existing steel railway bridges: Field test and numerical simulation. *Advances in Structural Engineering,* 21**,** 809-823.

MCGRATH, T. J., SELIG, E. T. & BEACH, T. J. 1995. Structural Behavior of Three-Sided Arch Span Bridge. *Transportation Research Record,* 1541.

MINISTERIO DE FOMENTO - DIRECCION GENERAL DE CARRETERAS 1999. Recomendaciones para la realizacion de pruebas de carga de recepcion en puentes de carretera.

MORDAK, A. G. & MANKO, Z. 2008. Static Load Tests of Posttensioned, Prestressed Concrete Road Bridge over Reservoir Water Plant. *Transportation Research Record,* 2050**,** 90-97.

MYERS, J. J., HOLDENER, D. & MERKLE, W. 2012. Load Testing and Load Distribution of Fiber Reinforced, Polymer Strengthened Bridges: Multi-year, Post Construction/Post Retrofit Performance Evaluation. *FRP Composites and Sustainability: Focusing on Innovation, Technology Implementation and Sustainability.* New York, NY.

NCHRP 1998. Manual for Bridge Rating through Load Testing. Washington, DC.

NCHRP 2014. NCHRP Synthesis 453 - State Bridge Load Posting: Processes and Practices. A synthesis of Highway Practice. Transportation Research Board.

NILIMAA, J., BLANKSVÄRD, T. & TALJSTEN, B. 2015. Assessment of concrete double-trough bridges. *Journal of Civil Structural Health Monitoring,* 2015**,** 29-36.

OHANIAN, E., WHITE, D. & BELL, E. S. 2017. Benefit Analysis of In-Place Load Testing for Bridges. *Transportation Research Board Annual Compendium of Papers***,** 14.

ORBAN, Z. & GUTERMANN, M. 2009. Assessment of masonry arch railway bridges using non-destructive in-situ testing methods. *Engineering Structures,* 31**,** 2287-2298.

PONTON, M. E., ROBALINO, A. F. & SANCHEZ, T. A. 2016. Stability Considerations for the Construction of Steel I-Girder Bridges using the Incremental Launching Method. *Annual Stability Conference Structural Stability Research Council.* Orlando, FL.

RIJKSWATERSTAAT 2013. Guidelines Assessment Bridges - assessment of structural safety of an existing bridge at reconstruction, usage and disapproval (in Dutch), RTD 1006:2013 1.1.

ROBALINO, A. F. & SANCHEZ, T. A. 2017. Global Lateral-Torsional Buckling of I-Girder Systems in Cantilever. *Proceedings, Annual Stability Conference, Structural Stability Conference, Structural Stability Research Council.* San Antonio, TX.

RUSSO, F. M., WIPF, T. J. & KLAIBER, F. W. 2000. Diagnostic Load Tests of a Prestressed Concrete Bridge Damaged by Overheight Vehicle Impact. *Transportation Research Record,* 1696**,** 103-110.

SANAYEI, M., REIFF, A. J., BRENNER, B. R. & IMBARO, G. R. 2016. Load Rating of a Fully Instrumented Bridge: Comparison of LRFR Approaches. *Journal of Performance of Constructed Facilities,* 2016**,** 2.

SANCHEZ, T. A., LAVIOLETTE, M. & FIALLO, M. 2017. Construction of Ecuador's First Launched Steel Girder Bridge. *Proceedings, The International Bridge Conference, Engineers' Society of Western Pennsylvania.* National Harbor, MD.

SANCHEZ, T. A., ROBALINO, A. F. & GRACIANO, C. Interaction Between Patch Loading, Bending, and Shear in Steel Girder Bridges Erected with the Incremental Launching Method. Proceedings, Annual Stability Conference, Structural Stability Conference, Structural Stability Research Council, 2018 Baltimore, MD.

SARAF, V. K. 1998. Evaluation of Existing RC Slab Bridges. *Journal of Performance of Constructed Facilities,* 12**,** 20-24.

TAYLOR, P., HOSTENG, T., WANG, X. & PHARES, B. 2016. Evaluation and Testing of a Lightweight Fine Aggregate Concrete Bridge Deck in Buchanan County, Iowa.

TAYLOR, S. E., RANKIN, B., CLELAND, D. J. & KIRKPATRICK, J. 2007. Serviceability of bridge deck slabs with arching action. *Aci Structural Journal,* 104**,** 39-48.

VELÁZQUEZ, B. M., YURA, J. A., FRANK, K. H., KREGER, M. E. & WOOD, S. L. 2000. Diagnostic load tests of a reinforced concrete pan-girder bridge. Austin, TX, USA: The University of Texas at Austin.

WIPF, T. J., RITTER, M. A. & WOOD, D. L. 2000. Evaluation and Field Load Testing of Timber Railroad Bridge. *Transportation Research Record,* 1696**,** 323-333.

YANG, Y. & MYERS, J. J. 2003. Live-Load Test Results of Missouri's First High-Performance Concrete Superstructure Bridge. *Transportation Research Record,* 1845**,** 96-103.

APPENDIX A: DETERMINATION OF EXPERIMENTAL RATING FACTOR ACCORDING TO BARKER

In Barker's method, the experimental rating at the inventory level *Exp_INV* is based on the separate effects that cause differences between the actual structure and the analytical model, and expressed as the ratio of the experimental rating factor at the inventory level *Exp_INV* to the analytical rating factor at the inventory level *Ana_INV*:

$$\frac{Exp\_INV}{Ana\_INV} = \left[\left(\frac{I_{mA}}{I_{mE}}\right)\left(\frac{M_E}{M_T}\right)\left(\frac{M_{LE}}{M_E}\right)\left(\frac{DF_A}{DF_E}\right)\left(\frac{M_{WL}}{\frac{M_{LE}}{DF_E}\frac{M_{RVW}}{M_{TRK}}}\right)\left(\frac{S_A^{ADIM}}{S_A}\right)\left(\frac{S_E}{S_A^{ADIM}}\right) \right] \quad (1)$$

The factor $\frac{I_{mA}}{I_{mE}}$ represents the contribution from the impact factor, with I_{mA} the analytical impact factor and I_{mE} the experimental impact factor. The value of the impact factor I_{mE} is determined in the field whereas I_{mA} is calculated based on the AASHTO impact factor (American Association of State Highway and Transportation Officials 2011). The effect of the measured impact factor can only be taken into account if the field test can cover the representative effect of different truck configurations and weights. The ratio $\frac{M_E}{M_T}$ represents the contribution from bearing restraint force effects, with M_E defined as the elastic measured moment with the bearing restraint moments removed, and M_T the experimental total moment, which, for steel-concrete composite bridges is the sum of the bending moment about the neutral axis of the steel girder M_L, the bending moment about the neutral axis of the concrete deck, M_U, and a force couple representing the interaction composite action $N \times a$. The factor $\frac{M_{LE}}{M_E}$ represents the contribution from longitudinal distribution of moment, with M_{LE} the experimental elastic moment adjusted for longitudinal distribution and M_E the elastic measured moment as discussed previously. The factor $\frac{DF_A}{DF_E}$ gives the contribution from lateral load distribution, with DF_A the analytical distribution factor and DF_E the distribution factor in the experiment. The factor $\frac{M_{WL}}{\left(\frac{M_{LE}}{DF_E}\right)\left(\frac{M_{RVW}}{M_{TRK}}\right)}$ takes into account the contribution from additional system stiffness, with M_{WL} the analytical wheel line moment for the RVW (rating vehicle weight) truck, M_{LE} the experimental elastic moment adjusted for longitudinal distribution, DF_E the experimental distribution factor, M_{RVW} the analytical wheel line RVW truck moment, and M_{TRK} the analytical wheel line test truck moment. The ratio M_{RVW}/M_{TRK} compares the actual test truck response to an equivalent rating response, so that M_{RVW} can produce ratings for any analytical rating vehicle. The factor $\frac{S_A^{ADIM}}{S_A}$ gives the contribution from actual section dimensions for section modulus, with S_A^{ADIM} the analytical section modulus with actual measured dimensions and S_A the analytical section modulus with design dimensions. Similarly, the factor $\frac{S_E}{S_A^{ADIM}}$ accounts for the contribution from unintended or additional composite action, with S_E the experimental section modulus.

The experimental lateral load distribution factor is the percentage of total moment resisted by an individual girder, and can be determined as follows:

$$DF_E = \frac{2\left(\sigma_i S_{Ai}\right)_{CriticalGirder}}{\Sigma\left(\sigma_i S_{Ai}\right)} \tag{2}$$

with σ_i the bottom flange stress for girder i and S_{Ai} either the actual section modulus or the nominal design section modulus for girder i.

To determine M_E and M_{LE}, the resulting moments in the test need to be analyzed, and different contributions need to be separated. The external moment at the support $M_{ext,sup}$ can be determined based on the measured strains and calculated stresses on the girders. When the stresses are known, the bearing force at an abutment $F_{bearing}$ is determined as:

$$F_{bearing} = A_{bf}\sigma_{bf} \tag{3}$$

with A_{bf} the area of the bottom flange at the bearing, and σ_{bf} the measured stress on the bottom flange at the bearing. A bearing force $F_{bearing}$ at a pier requires taking into account the girders on both sides of the support:

$$F_{bearing} = \frac{\left(\sigma_{bf}^{pier2} - \sigma_{bf}^{pier1}\right)A_{bf}}{2} \tag{4}$$

with σ_{bf}^{pier1} and σ_{bf}^{pier2} the measured stresses on the left and right side of the bearing. The external moment at the support, $M_{ext,sup}$, is then determined as:

$$M_{ext,\sup} = F_{bearing} \times d_{NA} \tag{5}$$

with d_{NA} the depth of the neutral axis. When $M_{ext,sup}$ is known, the actual shape of the bending moment diagram is known to determine the factor $\frac{M_{LE}}{M_E}$. Assuming a constant moment of inertia in all spans, the moment distribution can be determined was follows:

$$DM = \frac{\left(\frac{1}{L_i}\right)_{Critical\_Span}}{\Sigma\left(\frac{1}{L_i}\right)} \tag{6}$$

with DM the moment distribution factor, and L_i the span length on each side of the pier. Linear interpolation between the moments at the piers is used to find the bearing restraint moment M_{BR} at the critical section:

$$M_{BR}^{Critical\_Section} = \frac{M_{BR}^{Pier\#1} + M_{BR}^{Pier\#2}}{2} \tag{7}$$

To find the total experimental moment M_T, the bending moment about the steel neutral axis M_L is necessary, for which the stresses in the girder need to be determined. When strain gages are placed over the height of a girder, the strain distribution can be derived based on linear interpolation. The stress profile in the girder, including the axial bearing restraint stress, σ^{wa}, is then calculated as:

$$\sigma^{wa} = -\frac{1}{Sl}d + \frac{Int}{Sl} \tag{8}$$

with *Int* the neutral axis from the bottom flange, *Sl* the slope of the stress profile, *d* the depth from the bottom flange. The axial stress from the bearing force σ_{axial} can be removed as follows:

$$\sigma_{axial} = \frac{BF}{A_{comp}} \tag{9}$$

with *BF* the bearing force and A_{comp} the equivalent composite area:

$$A_{comp} = A_{girder} + \frac{A_{Conc}}{n} \tag{10}$$

with A_{girder} the nominal or measured area of the steel girder section, A_{Conc} the nominal or measured area of the concrete deck, and *n* the modular ratio when A_{girder} is determined for a steel girder. Now, the effect of the bearing axial force can be removed from the stress profile as follows:

$$\sigma = -\frac{1}{Sl}d + \frac{Int}{Sl} - \sigma_{axial} \tag{11}$$

The experimental total moment M_T can be divided into three components (see Figure 18):

1. bending moment about the steel neutral axis, M_L
2. bending moment about the concrete neutral axis, M_U
3. a couple representing the interaction composite action, $N \times a$

In other words, for steel girders with a concrete deck:

$$M_T = M_L + M_U + N \times a \tag{12}$$

$$M_L = \left(\sigma_0 - \sigma_{CG}\right) S_{steel}^{ADIM} \tag{13}$$

$$M_U = \frac{\left(E_{conc} I_{conc}\right)}{\left(E_{steel} I_{Steel}^{ADIM}\right)} M_L \tag{14}$$

$$N \times a = \sigma_{CG} A_{steel}^{ADIM} \times a \tag{15}$$

with σ_0 the stress at bottom flange calculated with Eq. (11), σ_{CG} the stress at the steel centroid calculated with Eq. (11), d_{CG} the depth of the steel centroid from the bottom flange using the measured dimensions, E_{conc} the Young's modulus of the concrete, E_{steel} the Young's modulus of the steel, I_{conc} the moment of inertia of the concrete slab, I_{steel}^{ADIM} the moment of inertia of the steel girder using measured dimensions, A_{steel}^{ADIM} the area of the steel girder using measured dimensions, and *a* the moment arm between the centroids of the steel girder and the concrete deck.

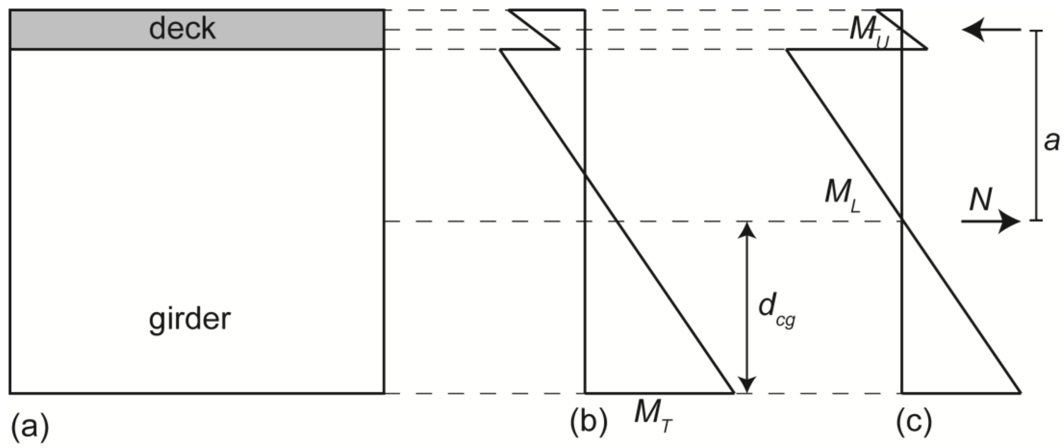

Figure 18. Total experimental moment, modified from (Barker 2001): (a) composite section; (b) measured bending moments M_T; (c) elastic moments M_E.

The elastic moments M_E with bearing restraint axial forces and bearing restraint moments M_{BR} removed are:

$$M_E = M_T - M_{BR} \tag{16}$$

The experimental section modulus S_E equals:

$$I_{Exp} = -\left(M_T\right) Sl \tag{17}$$

$$S_E = \frac{I_{Exp}}{Int} \tag{18}$$

The elastic longitudinal adjusted moment M_{LE} represents the elastic moment that should be at the section if the experimental longitudinal distribution would equal the moment from the analytical rating. The experimental moment diagram can be constructed with three measurement points, and compared to the analytical moment diagram under the same truck load:

$$STAT_A = M_C^2 - \left(1-\alpha\right) M_C^1 - \alpha M_C^3 \tag{19}$$

$$STAT_E = M_E^2 - \left(1-\alpha\right) M_E^1 - \alpha M_E^3 \tag{20}$$

with superscripts 1, 2, and 3 to denote the point at the left support, at the maximum span moment, and at the right support, respectively, $STAT_A$ the analytical static moment for the load truck, $STAT_E$ the static moment from the experiment, M_c the analytical moment at left, α, and right sections, and α the percentage of length to the point of maximum moment, i.e. the distance from point 1 to point 2 divided by the distance from point 1 to point 3. The longitudinal adjustment moment at the critical section is then:

$$M_{LE} = \frac{STAT_E}{STAT_A} M_C^2 \tag{21}$$

with M_C^2 the analytical moment at the section with the largest span moment (point number 2).

The ratio from Eq. (1) can be used for improving analytical ratings determined from hand calculations or spreadsheets, by programming the procedures introduced in this section.